13 Mar 1991, 1:30 pm - 3:30 pm

Lateral Stiffness and Damping Coefficient of Soils for Seismic Analysis of Buried Pipelines

Xinjian Zhang
Wuyi University, China/ Old Dominion University, Norfolk, VA

Leon R. L. Wang
Old Dominion University, Norfolk, VA

Isao Ishibashi
Old Dominion University, Norfolk, VA

Proceedings: Second International Conference on Recent Advances in Geotechnical Earthquake Engineering and Soil Dynamics, March 11-15, 1991, St. Louis, Missouri, Paper No. 5.25

Lateral Stiffness and Damping Coefficient of Soils for Seismic Analysis of Buried Pipelines

Xinjian Zhang, Lecturer, Civil Engineering Department, Wuyi University, Jiangmen, Guangdong, China, Visiting Scholar, ODU, Norfolk, Virginia

Leon R.L. Wang, Professor, Department of Civil Engineering, Old Dominion University, Norfolk, Virginia 23529

Isao Ishibashi, Professor, Department of Civil Engineering, Old Dominion University, Norfolk, Virginia 23529

SYNOPSIS: The stiffness and damping coefficient of soil are critical parameters in the Winkler's model for the seismic analysis of buried pipelines. This paper presents an analytical study in calculating the lateral dynamic stiffness(elastic and inelastic) and damping coefficient of soils for the seismic analysis of buried pipelines. The effects of the depth of the buried pipeline and the variation of Poisson's ratio of soils are considered. In the analysis, first, by using the elastic half-space theory, the elastic stiffness and geometrical damping coefficient of soils are obtained. From the numerical results, the elastic stiffness and geometrical damping coefficient by using best fitted formulas are presented. Secondly, empirical inelastic characteristics of soils are considered. The empirical data includes relationships among dynamic shear modulus, material damping ratio, and dynamic shear strain amplitude. The total damping coefficient of the system can be obtained by adding the material damping to the geometrical damping coefficient.

INTRODUCTION

Buried pipelines such as water/sewer distribution systems and oil and gas pipelines have been heavily damaged during past earthquakes. Because of the importance of lifelines to the health and safety of the populace, many analytical studies on the response behavior of buried pipelines due to earthquakes have been carried out. Most of the studies are based on the Winkler's model. In the model, the effects of the soil surrounding the pipeline are substituted by a series of springs and dashpots which represent the dynamic stiffness and damping of the soil. Since the soil properties of the surrounding medium play an important role in response characteristics of pipeline systems, an adequate estimation of dynamic stiffness and damping coefficient of soils in the Winkler's model is very essential.

For the seismic analysis of buried pipelines, very limited information on the dynamic stiffness and especially on the damping coefficient of soils is available. For the lateral stiffness of soil, k_{sl}, O'Rourke and Wang(1978) proposed $k_{sl} = 3G$, where G is the dynamic shear modulus of soils. From experiments on pipeline systems, Singhal and Meng(1983) proposed $k_{sl} = 9.51 \times 10^4$ psi (6.56×10^5 kN/m^2). These results are very approximate and the effects of the depth of the buried pipeline and Poisson's ratio were not considered. Trautmann and O'Rourke(1983) carried out model experiments on buried pipelines with different depth to diameter ratio H/D from 2 to 11.5. The experimental results showed that the lateral stiffness k_{sl} of soil increased with the increase of the depth to diameter ratio H/D both in medium sand and in dense sand. They concluded that the effect of the depth on k_{sl} can not be negalected. Parmelee and Ludtke(1975) presented a formula of calculating the stiffness of soil by integrating Mindlin's three dimensional solution. In the formula, the effect of the depth of the buried pipeline was considered. However, only the case of Poisson's ratio $\nu = 0.5$ was considered.

All of the stiffness described above are from static calculations. Novak and Nogami(1978) presented formulas of calculating the dynamic stiffness and damping coefficient of soils by using the elastodynamic infinite-space theory. However, the effect of the buried depth of the pipeline was not considered. Up till now, formulas of calculating the dynamic stiffness and damping coefficient of soil to include the effects of both of the buried depth of the pipeline and the change of Poisson's ratio for the seismic analysis of buried pipelines are still not available.

The objective of this paper is to present a rational method for evaluating the dynamic coefficients which characterize interacting forces at the interface between a buried pipeline and the surrounding medium. Based on the assumptions of the plane-strain conditions for the elastic medium surrounding the pipeline, the elastic stiffness and geometrical damping coefficient of soils are first obtained by using the elastodynamic half-space theory. Substituting the inelastic characteristics of soils obtained in laboratory dynamic experiments into the elastic stiffness and geometrical damping coefficient formulas and adding the material damping to the geometrical damping, the dynamic stiffness and damping coefficient are obtained which can be used to analyze the non-elastic seismic responses of buried pipelines.

ELASTIC STIFFNESS AND GEOMETRICAL DAMPING COEFFICIENT

Basic Considerations

When the buried pipeline in the soil is subjected to vibrations, the pipeline is resisted by the surrounding soil medium. The

resistance includes two parts: spring resistance and damping resistance. The former is a reaction force supplied by the surrounding soil medium which is proportinal to the displacement of the pipeline and can be expressed as $R_k = k \cdot u$, where u is the dynamic displacement of the pipeline, k is the spring constant of the soil in Winkler's model. The latter can be divided into two kinds of damping resistance: The geometrical damping resistance and material damping resistance. Geometrical damping resistance is due to the energy dissipation in the half-space, and the material damping resistance is due to inelastic properties of the soil medium surrounding the pipeline. In this section, an elastic soil medium with shear modulus G, Poisson's ratio ν and mass density ρ is assumed, and hence there only exists the elastic spring resistance and geometrical damping resistance in the system at this stage.

An assumption of the plane-strain is made to simplify the problem. Since it is difficult to consider accurately the interaction between the pipeline and the surrounding soil due to random earthquake vibration signals, a harmonic line load $P_o e^{-i\omega t}$ acting horizontally at the center of the pipe is used to simulate the interaction problem as shown in Fig. 1. Under the action of the dynamic loading, the horizontal displacement response u at point B is obtained and is taken as the average displacement response at the circumference of the pipe as done by Parmelee and Ludtke(1975). With the applied load $P_o e^{-i\omega t}$ and the displacement response u, the lateral complex stiffness K_{slc} of the soil is obtained as follows:

$$K_{slc} = \frac{P_o e^{-i\omega t}}{U} = K_{slr} + i K_{sli} \tag{1}$$

where K_{slr} is the real part of K_{slc}, which is the spring constant of the soil in Winkler's model, and K_{sli} is the imaginary part of K_{slc}, which is attributed to the energy dissipation in the half-space. From the energy dissipation, the geometrical damping coefficient can be obtained from K_{sli}.

Dynamic Responses of the Half-Space with a Buried Line Load Source

First, the buried horizontal harmonic line load source $P_o e^{-i\omega t}$ is considered. For any elastic system, when it is subjected to a harmonic source, the responses of the system also will be harmonic. Therefore, the displacement responses at any point in the half-space due to $P_o e^{-i\omega t}$ can be expressed as follows:

$$\left.\begin{aligned} u &= u^* e^{-i\omega t} \\ v &= v^* e^{-i\omega t} \end{aligned}\right\} \tag{2}$$

where u, v are the horizontal and vertical displacement responses at point (x,z), respectively, and u^*, v^* are the amplitudes of u, v, respectively. To obtain the solutions of u^*, v^* of the half-space due to a buried load, Image Method is used. As seen in Fig. 2, the solutions u_1^*, v_1^* at point (x,z) in the infinite-space due to the load $P_o e^{-i\omega t}$ which acts at point (0,h) are obtained first. Next, an imaginary load $-P_o e^{-i\omega t}$ is applied at point (0,-h) and the solutions u_2^*, v_2^* at point (x,z) in the infinite-space due to the imaginary load are obtained. Lastly, $-\sigma_z$ and $-\tau_{xz}$ are applied at z = 0 plane, where σ_z and τ_{xz} are the normal stress and the shear stress on the z = 0 plane induced by loads $P_o e^{-i\omega t}$ and $-P_o e^{-i\omega t}$ acting at points (0,h) and (0,-h) respectively in the infinite-space. The solutions at point (x,z) in the half-space due to $-\sigma_z$ and $-\tau_{xz}$ are obtained as u_3^*, v_3^*. The response amplitudes u^*, v^* at point (x,z) in the half-space due to the buried load $P_o e^{-i\omega t}$ are the sums of the above terms, respectively, as follows:

$$\left.\begin{aligned} u^* &= u_1^* + u_2^* + u_3^* \\ v^* &= v_1^* + v_2^* + v_3^* \end{aligned}\right\} \tag{3}$$

The method described above is called Image Method, which satisfies the boundary conditions (free ground surface) of the half-space problem along z = 0, that is, $\sigma_z = 0$, $\tau_{xz} = 0$.

As shown in Fig. 2, when a harmonic load $P_o e^{-i\omega t}$ acts at point (0,h) in the infinite-space, the responses at point (x,z) were given by Achenbach(1982) as follows:

$$\left.\begin{aligned} u_1^* &= \frac{i P_o}{4G}\left\{\frac{1}{K_T^2}\left[-H_o^{(1)}(K_L r) + H_o^{(1)}(K_T r)\right]_{xx} + H_o^{(1)}(K_T r)\right\} \\ v_1^* &= \frac{i P_o}{4G}\cdot\frac{1}{K_T^2}\left[-H_o^{(1)}(K_L r) + H_o^{(1)}(K_T r)\right]_{xz} \end{aligned}\right\} \tag{4}$$

in which, $H_o^{(1)}(x)$ is the first kind of Hankel function and zero order, and K_L, K_T are defined as follows:

$$\left.\begin{aligned} K_L^2 &= \frac{\rho}{\lambda + 2G}\cdot\omega^2 \\ K_T^2 &= \frac{\rho}{G}\cdot\omega^2 \end{aligned}\right\} \tag{5}$$

Due to the imaginary load $-P_o e^{-i\omega t}$ acting at point (0,-h), the responses at point (x,z) can be obtained similarly as:

$$\left.\begin{aligned} u_2^* &= -\frac{i P_o}{4G}\left\{\frac{1}{K_T^2}\left[-H_o^{(1)}(K_L r') + H_o^{(1)}(K_T r')\right]_{xx} + H_o^{(1)}(K_T r')\right\} \\ v_2^* &= -\frac{i P_o}{4G}\cdot\frac{1}{K_T^2}\left[-H_o^{(1)}(K_L r') + H_o^{(1)}(K_T r')\right]_{xz} \end{aligned}\right\} \tag{6}$$

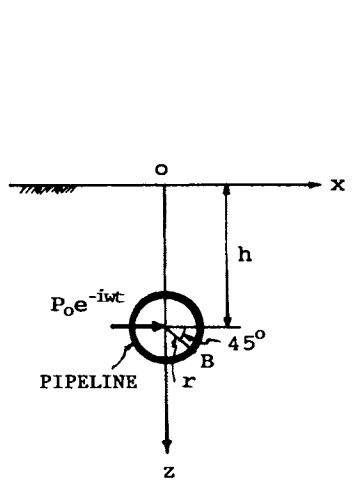

Fig. 1

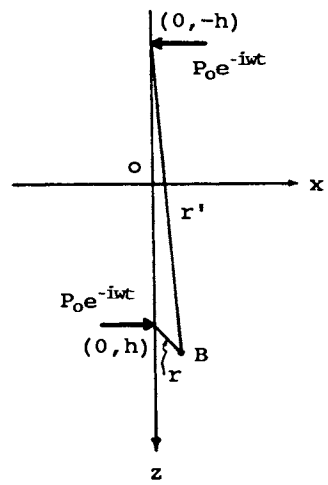

Fig. 2

where r, r' are the distances from points (0,h), (0,-h) to point (x,z), respectively, shown in Fig. 2.

With the solutions u_1^*, v_1^*, u_2^* and v_2^*, the stresses σ_z and τ_{xz} at the z = 0 plane can be obtained. The responses u_3^* at point (x,z) in the half-space due to $-\sigma_z$, $-\tau_{xz}$ can be obtained by using the elastodynamic half-space theory (Achenbach, 1973; Bath, 1968; Eringen and Suhubi, 1975; Ewing and Jardetzky, 1957). Accordingly, the horizontal response u^* at point (x,z) in the half-space due to the buried horizontal harmonic line load $P_o e^{-i\omega t}$ acting at point (0,h) is obtained as follows:

$$u^* = \frac{P_o}{2\pi G}\int_{-\infty}^{\infty} \frac{1}{K_T^2}\{\frac{\xi^2}{2\alpha}(e^{-\alpha|h-z|} - e^{-\alpha(h+z)}) - \frac{\beta}{2}\cdot (e^{-\beta|h-z|} - e^{-\beta(h+z)}) + \frac{1}{F(\xi)}[2\xi^2\beta(-2\xi^2 e^{-\alpha h} + (2\xi^2 - K_T^2)e^{-\beta h})\cdot e^{-\alpha z} - \beta(2\xi^2 - K_T^2)\cdot (-2\xi^2 e^{-\alpha h} + (2\xi^2 - K_T^2)e^{-\beta h})\cdot e^{-\beta z}]\}\cdot e^{-i\xi x}\, d\xi \quad (7)$$

in which, $F(\xi)$ is called Reyleigh Equation and is defined as:

$$F(\xi) = (2\xi^2 - K_T^2)^2 - 4\xi^2\alpha\beta \quad (8)$$

α and β are defined as:

$$\left.\begin{aligned}\alpha &= \sqrt{\xi^2 - K_L^2}\\ \beta &= \sqrt{\xi^2 - K_T^2}\end{aligned}\right\} \quad (9)$$

As shown above, Eq. 7 is an integral solution of u, and is not easily solved espcially for the field near the source. To evaluate the integration, Cagniard's method is used. Cagniard's method is a very useful method for the transient response analysis of the half-space due to a buried source (Achenbach, 1973, 1982; Bath, 1968; Eringen and Suhubi, 1975; Ewing and Jardetzky, 1957; Garvin, 1956; Lapwood, 1950; Pilant, 1979).

Before using Cagniard's method, it is necessary to change Eq. 7 to the Laplace transform of u. Eq. 7 is actually the Fourier transform of u over time t, and by substituting the frequency ω in Eq. 7 with -ip, and by changing the integral range $(-\infty, \infty)$ to $(0, \infty)$, the Laplace transform of u can be obtained. Then, by using Cagniard's method, the complex integral variable ξ in the Laplace transform is mapped onto a complex variable plane t, and the δ pulse responses of u are obtained. Fig. 3 shows a diagram of wave paths when the source and the receiving points are in the half-space.

As shown in Fig. 3, there generally exist six kinds of waves travelling from a buried source to a buried receiving point in the half-space. Those are the direct longitudinal wave, **P**, direct shear wave, **S**, reflected longitudinal wave of the longitudinal wave, **PP**, reflected longitudinal wave of the shear wave, **SP**, reflected shear wave of the longitudinal wave, **PS**, and reflected shear wave of the shear wave, **SS**. In the situation studied in this paper, as the receiving point is very close to the source, the reflecting coefficient of waves **SP**, **PS** are also very small. Therefore, waves **SP** and **PS** have no significant effect on the δ pulse responses u_δ

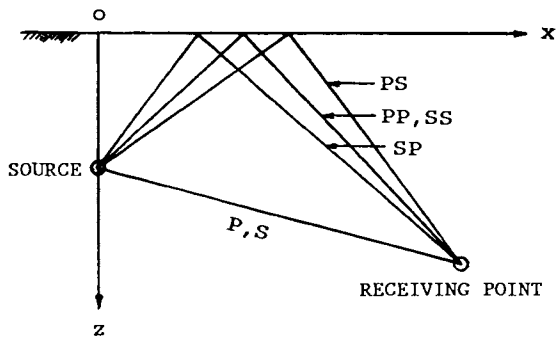

Fig. 3 Wave Paths in the Half-Space

(t) at the receiving point. Furthermore, $u_\delta(t)$ at the receiving point has four singular points which correspond to the arriving times t_p(= r/Vp), t_s(= r/Vs), t_{PP}(= r'/Vp) and t_{SS}(= r'/Vs) of waves **P**, **S**, **PP** and **SS**.

With the δ pulse response $u_\delta(t)$, the Laplace transform u^o of u can be obtained by using the following numerical integration equation:

$$u^o(\bar{p}) = P_o\sum_{i=0}^{\infty} u_\delta(\bar{t}_i)\cdot e^{-\bar{p}\cdot\bar{t}_i}\cdot\Delta\bar{t} \quad (10)$$

in which, $\bar{p}$ and $\bar{t}$ are dimensionless frequency and time, respectively, and are defined as follows:

$$\left.\begin{aligned}\bar{p} &= \frac{p\,r}{V_s}\\ \bar{t} &= \frac{t\cdot V_s}{r}\end{aligned}\right\} \quad (11)$$

In the above numerical integration computation, a special care should be paid to select the integration time step $\Delta\bar{t}$. As pointed out above, δ pulse response $u_\delta(t)$ has four singular points, at which $u_\delta(t)$ will become infinite, so that it is necessary to select $\Delta\bar{t}$ carefully to avoid these singular points. In this computation, the dimensionless integration time step $\Delta\bar{t}$ = 0.03 is selected.

According to the definition of the stiffness, the lateral elastic stiffness of the soil surrounding the pipeline is obtained from the Laplace transform $u^o(p)$ as follows:

$$K_e(\bar{p}) = \frac{P_o}{u^o(\bar{p})} \quad (12)$$

From the computations, it was found that the elastic stiffness $K_e(p)$ increased almost linearly with the increase of the dimensionless frequency $\bar{p}$ when $\bar{p} < 1.0$. For usual earthquake vibration analysis, $\bar{p}$ = 1.0, which corresponds to frequency f = 50 Hz when Vs = 150 m/s, r = 0.5 m, is high enough. Therefore, in this computation, a linear relation is established in the range of $\bar{p} \le 0.6$ as:

$$K_e(\bar{p}) = K + \bar{p}\cdot C_1 = 2\pi G(k + \bar{p}\cdot c) \quad (13)$$

where k and c are dimensionless factors.

As described before, a change in Eq. 13 from the Laplace transform to the Fourier transform can be made by taking $\bar{p} = i\bar{\omega}$, and by doing so, a complex elastic stiffness is obtained as follows:

$$K_e(\bar{\omega}) = 2\pi G(k + i\bar{\omega} \cdot c) \tag{14}$$

where $\bar{\omega}$ is a dimensionless frequency and is defined as:

$$\bar{\omega} = \frac{\omega r}{V_s} \tag{15}$$

The real part of K_e is the elastic stiffness of the soil surrounding the pipeline, and the imaginary part of K_e is attributed to the geometrical damping due to the energy dissipation in the half-space. When the pipeline moves with distance X laterally, the reaction of the soil to the pipeline will be R:

$$\begin{aligned} R &= K_e \cdot X \\ &= 2\pi G(k + i\bar{\omega} C) \cdot X \\ &= 2\pi G(k \cdot X + i\omega X \cdot \frac{r}{V_s} \cdot c) \\ &= 2\pi G(k \cdot X + \dot{X} \cdot \frac{r}{V_s} \cdot c) \\ &= K \cdot X + C \cdot \dot{X} \end{aligned} \tag{16}$$

in which, K is the lateral elastic stiffness of the soil surrounding the pipeline, and C is the geometrical damping coefficient. As can be seen in Eq. 16, the reaction of soil to a pipeline includes two parts: spring force $K \cdot X$, and viscous damping force $C \cdot \dot{X}$.

Numerical Analysis of Stiffness K and Geometrical Damping Coefficient C

Actually, the stiffness K and the geometrical damping coefficient C are related with several parameters of soil and pipeline, such as the shear modulus G, Poisson's ratio ν of soils, the depth to diameter ratio h/r, etc. From Eq. 16, K and C can be obtained as:

$$\left.\begin{aligned} K &= 2\pi G \cdot k \\ C &= 2\pi r \cdot \sqrt{G\rho} \cdot c \end{aligned}\right\} \tag{17}$$

where k and c are the dimensionless stiffness and the damping coefficient of soils which are only related to the depth to diameter ratio h/r and Poisson's ratio ν. k and C values for a range of h/r = 6 ~ 40 and ν = 0.1 ~ 0.4 were calculated and the results are shown in Figs. 4 and 5.

From Figs. 4 and 5, the following observations can be made. With the increase of the depth to diameter ratio h/r, stiffness k increases. For small h/r, the increase of k is more rapid, while for h/r>20, the increase of k is slow and reaches to a nearly constant value. On the other hand, geometrical damping coefficient c does not change very much with the depth to diameter ratio h/r. The higher the Poisson's ratio ν is, the larger k, and the larger c are obtained.

In the computations, the results of k and c for h/r<6.0 and Poisson's ratio ν close to 0.5 were omitted because of some calculation errors. When h/r<6.0, the complex equations in the δ pulse response equation are not in good balance, which led to calculation errors. And when Poisson's ratio ν is close to 0.5, the ratio of Vp/Vs becomes infinite, which also gave calculation errors.

With the numerical computation results by using curve fitting method, formulas of calculating k and c with any depth to diameter ratio h/r and Poisson's ratio ν are obtained as follows:

$$\left.\begin{aligned} k &= \frac{0.0252}{1.714 - \nu} \cdot e^{3.146\left(1 - \frac{r}{h}\right)} \\ c &= 2.049 \cdot e^{\frac{0.0562}{0.58 - \nu}} \end{aligned}\right\} \tag{18}$$

Then, by substituting k and c into Eq. 17, the elastic lateral stiffness K and geometrical damping coefficient C can be obtained:

$$\left.\begin{aligned} K &= \frac{0.0252}{1.714 - \nu} \cdot e^{3.146\left(1 - \frac{r}{h}\right)} \cdot 2\pi G \\ C &= 2.049 \cdot e^{\frac{0.0562}{0.58 - \nu}} \cdot 2\pi r \cdot \sqrt{G\rho} \end{aligned}\right\} \tag{19}$$

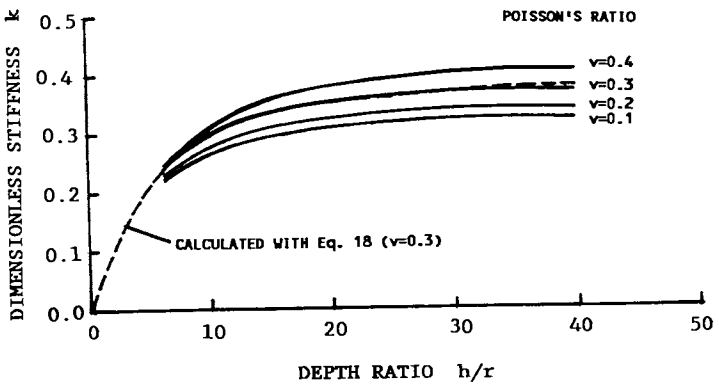

Fig. 4 k versus h/r with various ν

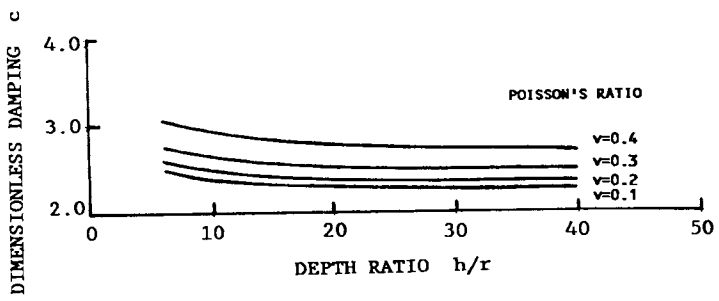

Fig. 5 c versus h/r with various ν

INELASTIC CHARACTERISTICS OF SOILS

Due to a strong nonlinearity of soils, the dynamic shear modulus G of soils decreases with the increase of the dynamic shear strain amplitude γ. And when soils are subjected to cyclic shear loadings, their stress-strain relationships are normally in the forms of hyteresis loops, which are attributed to the material damping D of soils.

Shear modulus G and the material damping D are the most important dynamic parameters of soils, which are affected by many factors such as cyclic shear strain amplitude γ, effective normal stress σ_o, void ratio e, plasticity index Ip, etc. With many experiments data for sands, Ishibashi(1981) and Khouri(1984) proposed formulas of calculating the average shear modulus G and material damping ratio D for sands as follows:

$$\left.\begin{aligned} \frac{G}{G_{max}} &= K(\gamma)\,\sigma_o^{m(\gamma)-m_o} \\ D &= 0.195\left(\frac{G}{G_{max}}\right)^2 - 0.515\left(\frac{G}{G_{max}}\right) + 0.333 \end{aligned}\right\} \quad (20)$$

in which,

$$\left.\begin{aligned} K(\gamma) &= 0.5\{1 + tanh[ln(\frac{0.0102}{\gamma})^{0.492}]\} \\ m(\gamma) - m_o &= 0.272\{1 - tanh[ln(\frac{0.0556}{\gamma})^{0.4}]\} \end{aligned}\right\} \quad (21)$$

σ_o is the mean effective normal stress (kN/m²), $\sigma_0 = (\sigma_{01} + \sigma_{02} + \sigma_{03})/3$, and γ is the cyclic shear strain amplitude in percent.

For clays, G/G_{max} increases with the increase of the plasticity index Ip, while the damping ratio D decreases(Dobry and Vucetic, 1987). No general formulations on G/G_{max} and D for clays are available at the present time due to lack of data.

INELASTIC STIFFNESS AND DAMPING COEFFICIENT OF SOILS

During earthquakes, the shear strain γ of soils is normally high. As the shear modulus G of soils changes with the shear strain γ of soils, the stiffness K of soils will also change. By substituting the above non-elastic relationship $G/G_{max} - \gamma$ into the equations of the stiffness K and geometrical damping coefficient C (Eq. 19), and adding the material damping ratio D to the geometrical damping coefficient C, the lateral inelastic stiffness K_{si} and damping coefficient C_{si} (the total damping coefficient) can be obtained.

Dynamic shear strain amplitude of soil at the depth of pipeline during earthquake, γ can be calculated according to the following equations (Toki et al., 1983):

$$\gamma = \frac{1}{\pi \cdot H} \cdot T \cdot S_v \cdot K_{oh} \cdot Sin\left(\frac{\pi h}{2H}\right) \quad (22)$$

where

H : thickness of surface layer (m);

S_v : velocity response spectrum per unit seismic intensity, which is determined from:

$$\left.\begin{aligned} S_v\,(m/sec) &= 2.50 \cdot T \quad for\ 0.1\ sec \le T < 0.6\ sec \\ &= 1.5 \quad for\ 0.6\ sec \le T \end{aligned}\right\} \quad (23)$$

K_{oh} : horizontal seismic intensity at base rock;

$$K_{oh} = 0.5 \cdot k_h \quad (24)$$

k_h : horizontal seismic intensity at ground surface (g).

T : natural period of surface layer (sec),

$$T = \frac{4H}{\bar{V}_s} \quad (25)$$

$\bar{V}_s$: average shear wave velocity of surface layer (m/sec).

When shear wave velocity was measured from elastic wave survey, the measured velocities shall be multiplied with 0.6 for sand, and 0.85 for clay.

When it is estimated from the standard penetration value N,

$$\left.\begin{aligned} \bar{V}_s &= 62\,N^{0.021} \quad for\ sands \\ &\quad 122\,N^{0.078} \quad for\ clays \end{aligned}\right\} \quad (26)$$

for multi-surface-layer with V_{si} as shear wave velocity for individual layer H_i:

$$\bar{V}_s = \frac{\sum V_{si} \cdot H_i}{\sum H_i} \quad (27)$$

CONCLUSIONS

The seismic soil-structure interaction of buried pipeline has been examined with a simplified model of the system. In this analysis, it was assumed that the action of pipeline in the soil during earthquakes can be considered as a horizontal line load which is normal to, and uniformally distributed along the longitudinal axis of the pipe.

In this analysis, first, by using the elastodynamics theory of the half-space, lateral elastic stiffness K and geometrical damping coefficient C of the soil for seismic analyses of buried pipeline were obtained. It was found that: (1) K and C do not change significantly with the change of frequency for a low frequency range (0 ~ 50 Hz) which covers the range for seismic analyses, (2) K increases with the increase of the depth to diameter ratio h/r of pipeline, and when h/r>20, K reaches to the maximum value and remains with the value thereafter, (3) the change of C with h/r is very small, and (4) both of K and C are very significantly affected by Poisson's ratio ν of the soil; the larger ν is, the bigger K and C were obtained.

Considering the inelastic characteristics of soils, non-elastic relationship formulas of $G/G_{max} - \gamma$ and the material damping ratio D were substituted into the elastic equations of K and C, and the lateral inelastic stiffness K and damping coefficient C were obtained. With the

increase of the shear strain γ of soil, K will decrease, so will the geometrical damping coefficient, while the material damping ratio D will increase. With the given lateral inelastic stiffness K and the damping coefficient C of the soil, the lateral non-elastic seismic response analysis of buried pipelines can be more accurately performed.

REFERENCES

Achenbach, J.D., "Wave Propagation in Elastic Solids," North- Holland Pub. Company, 1973.

Achenbach, J.D., "Ray Methods for Waves in Elastic Solids," Pitman Advanced Pub. Program, 1982.

Bath, M., "Mathematical Aspects of Seismiology," Elsevier Pub. Company, 1968.

Dobry, R. and Vucetic, M., "Dynamic Properties and Seismic Response of Soft Clay Deposits," Proceedings of International Symposium on Geotechnical Engineering of Soft soils, Mexico City, 1987, Vol.2, 51-87.

Eringen, A.C. and Suhubi, E.S., "Elastodynamics," Vol.2, Academic Press, 1975.

Ewing, W.M. and Jardetzky, W.S., "Elastic Waves in Layered Media," MacGraw-Hill Book Company, 1957.

Garvin, W.W., "Exact Transient Solution of the Buried Line Source Problem," Proceedings of Royal Society of London, Series A., 1956, Vol.234, 528-541.

Ishibashi, I., "Dynamic Soil Properties," Proceedings of the Joint U.S.-P.R.C. Microzonation Workshop, Harbin, China, 1981, 1-21/16.

Khouri, N.Q., "Dynamic Properties of Soils," Master thesis, Department of Civil Engineering, Syracuse University, 1984.

Lapwood, E.R., "The Disturbance due to a Line Source in a Semi-Infinite Elastic Medium," Philosophical Transactions of the Royal Society of London, Series A, 1950, Vol.242, 63-100.

Novak, M. and Nogami, T., " Dynamic Soil Reactions for Plane Strain Case," Journal of the Engineering Mechanics Division, ASCE, 1978, Vol.104, EM4, 953-961.

O'Rourke, M. and Wang, L.R.L., "Earthquake Response of Buried Pipeline," Proceedings on the Speciality Conference on Earthquake Engineering and Soil Dynamics, ASCE, Pasadena, CA., June, 1978, 720-731.

Parmelee, R.A. and Ludtke, C.A., "Seismic Soil-Structure Interaction of Buried Pipelines," Proceedings of the U.S. National Conference on Earthquake Engineering, Ann Arbor, June, 1975, 406-415.

Pilant, W.L., "Elastic Waves in the Earth," Elsevier Scientific Pub. Company, 1979.

Singhal, A.C. and Meng, C.L., "Stresses at Pipeline Joints," Earthquake Behavior and Safety of Oil and Gas Storage Facilities, Buried Pipelines and Equipment, PVP-Vol.77, ASME, June, 1983, 217-224.

Toki, K., Fukumori, Y., Sako, M. and Tsubakimoto, T., "Recommended Practice for Earthquake Resistant Design of High Pressure Gas Pipelines," Earthquake Behavior and Safety of Oil and Gas Storage Facilities, Buried Pipelines and Equipment, PVP-Vol.77, ASME, June, 1983, 349-356.

Trautmann, C.H. and O'Rourke, T.D., "Load-Displacement Characteristics of a Buried Pipe Affected by Permanent Earthquake Ground Movements," Earthquake Behavior and Safety of Oil and Gas Storage Facilities, Buried Pipelines and Equipment, PVP-Vol.77, ASME, June, 1983, 254-262.